Article

pH as a Trigger of Peptide β-Sheet Self-Assembly and Reversible Switching between Nematic and Isotropic Phases

Amalia Aggeli, Mark Bell, Lisa M. Carrick, Colin W. G. Fishwick, Richard Harding, Peter J. Mawer, Sheena E. Radford, Andrew E. Strong, and Neville Boden

J. Am. Chem. Soc., **2003**, 125 (32), 9619-9628• DOI: 10.1021/ja021047i • Publication Date (Web): 16 July 2003

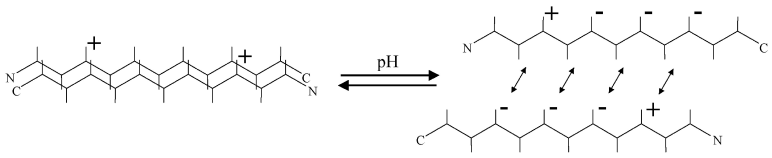

More About This Article

Additional resources and features associated with this article are available within the HTML version:

- Supporting Information
- Links to the 28 articles that cite this article, as of the time of this article download
- Access to high resolution figures
- Links to articles and content related to this article
- Copyright permission to reproduce figures and/or text from this article

View the Full Text HTML

J|A|C|S
ARTICLES
Published on Web 07/16/2003

pH as a Trigger of Peptide β-Sheet Self-Assembly and Reversible Switching between Nematic and Isotropic Phases

Amalia Aggeli,[†,‡] Mark Bell,[†] Lisa M. Carrick,[†] Colin W. G. Fishwick,[‡] Richard Harding,[†] Peter J. Mawer,[†] Sheena E. Radford,[§] Andrew E. Strong,[†] and Neville Boden*[,†,‡]

Contribution from the Centre for Self-Organising Molecular Systems, Department of Chemistry, and School of Biochemistry and Molecular Biology, University of Leeds, Leeds, LS2 9JT, U.K.

Received July 31, 2002; E-mail: n.boden@chemistry.leeds.ac.uk

Abstract: The hierarchical self-assembly of rationally designed synthetic peptides into β-sheet tapes, ribbons, fibrils, and fibers opens up potentially useful routes to soft−solidlike materials such as hydrogels, organogels, or liquid crystals. Here, it is shown how incorporation of Glu ($-CH_2CH_2COOH$) or Orn ($-CH_2CH_2CH_2NH_2$) into the primary structure of an 11 amino acid peptide enables self-assembly to be rapidly (seconds) and reversibly controlled by simply changing pH. Solutions of monomeric peptide, typically at concentrations in excess of 0.003 v/v, can be switched within seconds to, for example, nematic gel states comprised of interconnected orientationally ordered arrays of fibrils or vice versa. This is to be compared with the lyophilized peptide dissolution route to nematic fluids and gels which is impracticably long, taking many hours or even days. An important design principle, that stabilization of fibrillar dispersions requires of the order of one unit of net positive or negative charge per peptide molecule, is first demonstrated and then used to design an 11 amino acid peptide P_{11}-3 (CH_3CO-Gln-Gln-Arg-Phe-Gln-Trp-Gln-Phe-Gln-Gln-Gln-NH_2) whose self-assembly behavior is independent of pH ($1 < pH < 10$). pH control is then incorporated by appropriately positioning Glu or Orn side chains so that the peptide−peptide free energy of interaction in the tapelike substructure is strongly influenced by direct electrostatic forces between γ-COO^- in Glu^- or δ-NH_3^+ in Orn^+, respectively. This design principle is illustrated by the behavior of two peptides: P_{11}-4 (CH_3CO-Gln-Gln-Arg-Phe-Glu-Trp-Glu-Phe-Glu-Gln-Gln-NH_2) which can be switched from its nematic to its isotropic fluid state by increasing pH and P_{11}-5 (CH_3CO-Gln-Gln-Orn-Phe-Orn-Trp-Orn-Phe-Gln-Gln-Gln-NH_2) designed to exhibit the converse behavior. Acid−base titrations of fibrillar dispersions reveal deprotonation of the γ-COOH of Glu or of the δ-NH_3^+ of Orn^+ occurs over wide bands of up to 5 pH units, a feature of polyelectrolytes. The values of the energy parameters controlling self-assembly can therefore be smoothly and continuously varied by changing pH. This enables isotropic fluid-to-nematic transitions to be triggered by relatively small additions of acid or base, typically 1 part in 10^3 by volume of 1 M HCl or NaOH.

Introduction

An emergent activity is exploration of the prospects for exploiting peptide self-assembly as a route to novel soft−solid materials.[1] The motivation stems from the opportunities of, first, incorporating protein-like responsivity into the nanostructure to provide control over macroscopic properties and functionality and, second, producing materials from natural resources. One approach has been to exploit one-dimensional self-assembling properties of peptides to produce elongated β-sheet tapes.[2,3] The essential requirement is that the peptides have a propensity to form cross β-structures. However, it has recently been shown that the intrinsic chirality of peptides has a major impact on their self-assembly behavior.[4] This results in the formation of a hierarchy of supramolecular structures with increasing concentration, helical tapes (single molecule thick), twisted ribbons (double tapes), fibrils (twisted stacks of ribbons), and fibers (entwined fibrils) (Figure 1). Of practical interest, tapes and ribbons, which are relatively flexible, become entangled at concentrations of ca. 0.001 v/v to form viscoelastic solutions,[2,3] while fibrils and fibers, which are semirigid, can form nematic fluids at similar concentrations and elastomeric nematic gels at higher concentrations.[4] By appropriate choice of amino acids, this hierarchical self-assembly can be effected in either water or polar organic solvents leading to hydrogels[2−5] or organo-

[†] Centre for Self-Organising Molecular Systems, University of Leeds.
[‡] Department of Chemistry, University of Leeds.
[§] School of Biochemistry and Molecular Biology, University of Leeds.

(1) Self-Assembling Peptide Systems in Biology, Medicine and Engineering; Aggeli, A., Boden, N., Zhang, S., Eds.; Kluwer Academic Publishers, 2001.
(2) Aggeli, A.; Bell, M.; Boden, N.; Keen, J. N.; Knowles, P. F.; McLeish, T. C. B.; Pitkeathly, M.; Radford, S. E. *Nature* **1997**, *386*, 259−262.
(3) Aggeli, A.; Bell, M.; Boden, N.; Keen, J. N.; McLeish, T. C. B.; Nyrkova, I. A.; Radford, S. E.; Semenov, A. N. *J. Mater. Chem.* **1997**, *7* (7), 1135−1145.
(4) (a) Aggeli, A.; Nyrkova, I. A.; Bell, M.; Harding, R.; Carrick, L.; McLeish, T. C. B.; Semenov, A. N.; Boden, N. *Proc. Nat. Acad. Sci. U.S.A.* **2001**, *98*, 11857−11862. (b) Nyrkova, I.; Semenov, A.; Aggeli, A.; Boden, N. *Eur. Phys. J. B* **2000**, *17*, 481−497. (c) Nyrkova, I.; Semenov, A. N.; Aggeli, A.; Bell, M.; Boden, N.; McLeish, T. C. B. *Eur. Phys. J. B* **2000**, *17*, 499−513.

10.1021/ja021047i CCC: $25.00

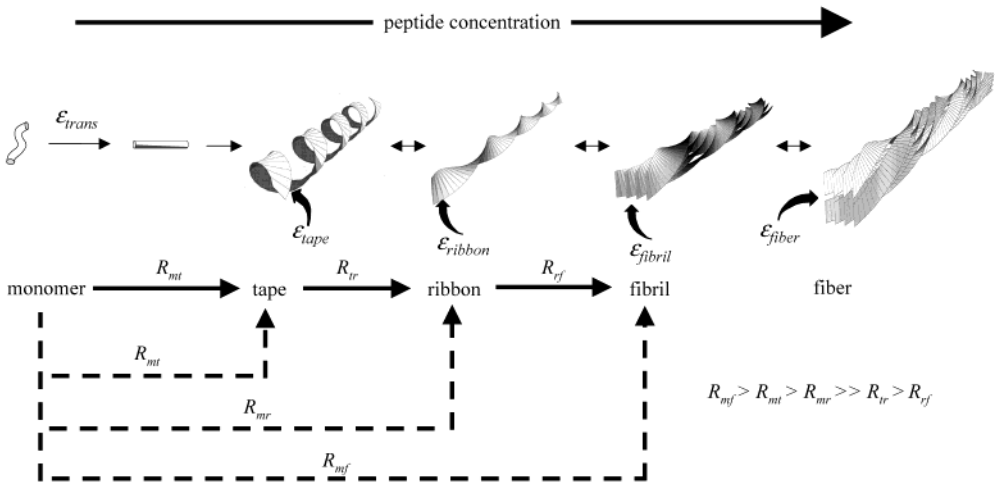

Figure 1. The global equilibrium configurations obtained by the hierarchical self-assembly of β-sheet forming peptides.[4] The set of energy parameters ϵ_j correspond to the free energy differences per peptide molecule between successive structures. The "critical" peptide concentrations at which each new configuration begins to appear is determined by the ϵ_j. The R_{ij} are the conversion rates both between and to the various configurations. The process depicted by solid arrows represents the dissolution route of lyophilized solid at constant pH, while the dashed arrows represent the direct and simultaneous conversion of monomer to tapes, ribbons, fibrils, and fibers when the respective critical concentrations governing their self-assembly are instantaneously switched by pH change to values above the absolute peptide concentration in solution. In principle, all of the transformations depicted will be reversible.

gels,[2,3] respectively. Thus, a wide variety of novel soft-matter-like materials, which are potentially biocompatible and biodegradable, could be produced via this route. However, it should be recognized that any chiral unit able to undergo one-dimensional self-assembly can in principle form fibrils and fibers, albeit tapes and ribbons are only predicted for chiral rodlike units of which peptides in their β-strand configuration are the archetypal example.[4] Indeed, there are a rich variety of synthetic chiral monomers which express this kind of behavior. Typical examples include complementary associating derivatives of tartaric acid[6] or of chiral 1,2-diaminocyclohexane with (*S*,*S*)-1,2-cyclohexanol[7] substituted porphyrins and phthalocyanines,[8] derivatives of carbohydrates[7] and cholesterol,[8,9] lithium salts of D (or L)-12-hydroxystearic acid,[8] *N*-*n*-octyl-D-gluconamide,[7,10] copper β-diketonates,[8] and chiral cyclohexanediamides.[11] These all give rise to fibrils with well-defined twist and dimensions and which have the propensity to form networks, gels, and liquid crystals. However, peptides tend to be exceptional in that they form tapes and ribbons, too. Nevertheless, work with peptides to date[12] has tended to be focused on fibrillar β-sheet networks.

Peptide-based materials offer unique materials' engineering opportunities,[1] apart from the more obvious one of being able to incorporate biological-like functionality. This can be appreciated by recognizing how accessibility of the peptide hierarchy of structures is determined by a set of energetic parameters ϵ_j (Figure 1). These govern the peptide concentration ranges over which particular structures are stable. Appropriate choice of amino acid side chains enables the magnitude of these ϵ_j to be modulated by structural changes brought about by external chemical, optical, or electrical triggers. This provides a mechanism for tuning the nanostrucutres of these aggregates or for switching from one macromolecular structure to another and, as a consequence, between associated macroscopic states of the system. This is of considerable practical utility in the processing of these materials as well as in their applications. Prospective applications of nematic hydrogels and organogels comprised of biologically functionalizable β-sheet fibrillar networks include matrixes for separation of large biomolecules such as proteins, scaffolds for cell growth, encapsulation and controlled release of drugs, templates for mineral growth, and so forth. However, here we focus on understanding how the control of structures and properties of these materials can be achieved simply by switching the pH of the solution. We exploit the fact that amino acid side chains terminated with $-COOH$ or $-NH_2$ groups can be in either a protonated or deprotonated state at pH values which are, respectively, below or above their nominal p*K* values. These side chains can, by design, be specifically located on the peptide chain so as to control the electrostatic interactions between neighboring peptides and to effectively dominate the association free energy per peptide−peptide "bond" ϵ_{tape} within tapelike aggregates. By way of illustrating this principle, we describe how an 11 amino acid peptide P_{11}-2 (Table 1), previously referred to as DN1,[3,4] can be modified so as to provide pH control over its self-assembly behavior. It has already been established[4] how, with increasing concentration in water at pH 2, P_{11}-2 associates successively into tapes, ribbons, fibrils, and finally fibers. Here, we report on the full pH dependence of the self-assembly behavior of this peptide.

Table 1. Peptide Primary Structures

P_{11}-2:	CH_3CO-Gln-Gln-Arg-Phe-Gln-Trp-Gln-Phe-Glu-Gln-Gln-NH_2
P_{11}-3:	CH_3CO-Gln-Gln-Arg-Phe-Gln-Trp-Gln-Phe-*Gln*-Gln-Gln-NH_2
P_{11}-4:	CH_3CO-Gln-Gln-Arg-Phe-*Glu*-Trp-*Glu*-Phe-Glu-Gln-Gln-NH_2
P_{11}-5:	CH_3CO-Gln-Gln-*Orn*-Phe-*Orn*-Trp-*Orn*-Phe-*Gln*-Gln-Gln-NH_2

(5) (a) Collier, J. H.; Hu, B. H.; Ruberti, J. W.; Zhang, J.; Shum, P.; Thompson, D. H.; Messersmith, P. B. *J. Am. Chem. Soc.* **2001**, *123*, 9463−9464. (b) Marini, D. M.; Hwang, W.; Lauffenburger, D. A.; Zhang, S.; Kamm, R. D. *Nano Lett.* **2002**, *2*, 295−299.
(6) Gulik-Krzywicki, T.; Fouquey, C.; Lehn, J. M. *Proc. Natl. Acad. Sci. U.S.A.* **1993**, *90*, 163−167.
(7) Rowan, A. E.; Nolte, R. J. M. *Angew. Chem., Int. Ed.* **1998**, *37*, 63−68.
(8) Terech, P.; Weiss, R. G. *Chem. Rev.* **1997**, *97*, 3133−3159.
(9) Murata, K.; Aoki, M.; Suzuku, T.; Harada, T.; Kawabata, H. *J. Am. Chem. Soc.* **1994**, *116*, 6664−6676.
(10) Fuhrhop, J.-H.; Helfrich, W. *Chem. Rev.* **1993**, *93*, 1565−1582.
(11) Hanabusa, K.; Yamada, M.; Kimura, M.; Shirai, H. *Angew. Chem., Int. Ed* **1996**, *35*, 1949−1951.
(12) (a) Lashuel, H. A.; LaBrenz, S. R.; Woo, L.; Serpell, L. C.; Kelly, J. W. *J. Am. Chem. Soc.* **2000**, *122*, 5262−5277. (b) Yamada, N.; Ariga, K.; Naito, M.; Matsubara, K.; Koyama, E. *J. Am. Chem. Soc.* **1998**, *120*, 12192−12199. (c) Burkoth, T. S.; Benzinger, T. L. S.; Jones, D. N. M.; Hallenga, K.; Meredith, S. C.; Lynn, D. G. *J. Am. Chem. Soc.* **1998**, *120*, 7655−7656. (d) Qu, Y.; Payne, S. C.; Apkarian, R. P.; Conticello, V. P. *J. Am. Chem. Soc.* **2000**, *122*, 5014−5015.

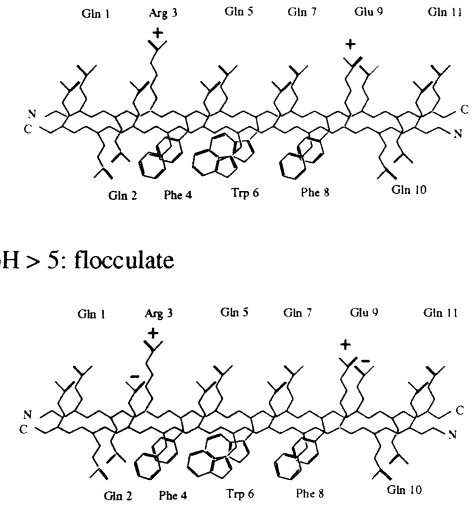

Figure 2. Electrostatic charge distribution on P_{11}-2 dimer in an antiparallel β-sheet tapelike substructure: (a) pH < 5 and (b) pH > 5.

The results reveal an important design principle, which is subsequently confirmed by the design of the peptide P_{11}-3 (Table 1) whose self-assembly behavior is shown to be independent of pH ($1 < pH < 10$). Against this background, the design principles for pH control of self-assembly are formulated and illustrated by the behavior of two peptides P_{11}-4 and P_{11}-5. P_{11}-4 can be switched from its supramolecular to monomeric state by increasing the pH, while the converse behavior is built into P_{11}-5.

Results

Requirements for Stable Dispersions of Fibrils. The primary structure of P_{11}-2 (Table 1) is based on a sequence of glutamine (Gln) residues, whose side chains interact strongly in water[13] via hydrophobic and complementary hydrogen bonding interactions to promote β-sheet formation (Figure 2). Arginine (Arg) and glutamic acid (Glu) residues in positions 3 and 9, respectively, were initially incorporated to provide molecular recognition between adjacent antiparallel β-strands in tapelike aggregates by complementary electrostatic interactions. The phenylalanine, tryptophan, and phenylalanine residues in positions 4, 6, and 8, respectively, also contribute to this intermolecular recognition, but their main purpose is to provide a hydrophobic "adhesive" stripe running along one face of the tape to promote association of tapes into ribbons in water. Indeed, in acid solution (pH 2), tapes comprised of 3−4 peptides are formed at low peptide concentrations before the growth of much longer (μm) ribbons takes over at peptide concentration $c \approx 0.09$ mM.[1] At $c \geq 0.6$ mM, ribbons associate into fibrils comprised of four ribbons, at $c \geq 0.9$ mM (0.001 v/v), a transition from an isotropic fluid to a nematic state occurs, and, at $c \geq 4$ mM (0.004 v/v), the birefringent solution of P_{11}-2 becomes a self-supporting nematic gel.

We have now extended our studies of P_{11}-2 to reveal that solutions at $c = 6.3$ mM form stable nematic gels at pH values less than 5. We believe this is because at these pH values the fibrils have a net positive charge (only Arg^+ is charged)[14] and this stabilizes the fibrillar dispersion (Figure 2a). At higher pH values, we observe that fibrils flocculate (Figure 2b) making the gel unstable. At pH values above 5, the γ-carboxyl group of Glu will be negatively charged rendering the peptide as a whole electrically neutral. The apparent pK value for terminal COOH or NH_3^+ groups on amino acid side chains in self-assembling peptides may differ significantly from the values of the free amino acid in solution (Glu 4.1; Arg 12.5) due to electrostatic interactions with neighboring charged side chains. We expected stable fibrillar dispersions would have been obtained at high pH values above the apparent pK of Arg^+. However, we find that the high ionic strength (high concentration of base) at these pH values leads to flocculation. Thus, it appears that to stabilize dispersions of fibrils requires of the order of one unit of net positive or negative charge per peptide molecule. To test this hypothesis, a new peptide P_{11}-3 (Table 1) was designed. The substitution Glu → Gln at position 9 leaves just a single ionizable arginine side chain which is expected to remain positively charged up to its pK (pH 12.5), and we hypothesized that this peptide would thus form stable fibrillar dispersions over a wide pH range. Indeed, this is what we observed. In 6.3 mM solutions, fibrils are obtained and give rise to nematic gels between $1 < pH < 10$. Flocculation occurs above pH 10, implying that the arginine is deprotonated 2.5 pH units lower than the free amino acid in solution. This shift in the apparent pK value possibly arises from electrostatic repulsion between positively charged guanido groups on nearby Arg^+ side chains.

Switching between Nematic Gel or Nematic Fluid at Low pH and Isotropic Fluid at High pH Values. Peptide P_{11}-4 was designed to form fibrils at low pH and to be monomeric in solution at high pH. Glutamic acid residues have been substituted for the glutamine residues in positions 5 and 7. The γ-carboxyl groups should be uncharged at pH ≤ 2.[14] As a consequence, there should be one net positive charge per peptide on Arg^+, and thus, we expect stable dispersions of fibrils. In contrast, at higher pH, all three carboxyl groups are expected to be deprotonated (negatively charged). The resulting electrostatic repulsive forces between adjacent $\gamma-COO^-$ groups in neighboring peptides should then severely attenuate the magnitude of the peptide−peptide energy of attraction ϵ_{tape} within the tapelike substructure, leading to fibril-to-monomer dissociation. In practice, more complex behavior is observed. In solutions of $c = 6.3$ mM, region I in Figure 3a, self-supporting birefringent gels are obtained within $2.0 < pH < 3.2$. Within $3.2 < pH < 5.0$ flocculation occurs (region II), while within $5.0 < pH < 7.0$, viscous birefringent nematic fluids prevail (region III). Nematic gels are only obtained at $c \geq 12.6$ mM in the pH range $5.0 < pH < 7.0$. At pH > 7.2, optically isotropic Newtonian fluids are observed (region IV). The optical micrograph (Figure 3b) for a solution at pH 3 shows a typical threadlike viscoelastic nematic texture.[4] Electron microscopy reveals semirigid, fibril-like structures at pH < 3.2 (Figure 3c), microns in length, with a left-handed twist about their long axis. Their widths are seen to vary between 4 and 30 nm, with 8 and 16 nm being most frequently observed. The IR spectrum (Figure 3d (upper trace)) has an intense band in the amide I′ region

(13) Perutz, M. F.; Johnson, T.; Suzuki, M.; Finch, J. T. *Proc. Natl. Acad. Sci. U.S.A.* **1994**, *91*, 5355−5358.

(14) Voet, D.; Voet, J. G. *Biochemistry, 2nd ed.;* John Wiley and Sons Inc.: New York, 1995; Chapter 4, pp 58−59.

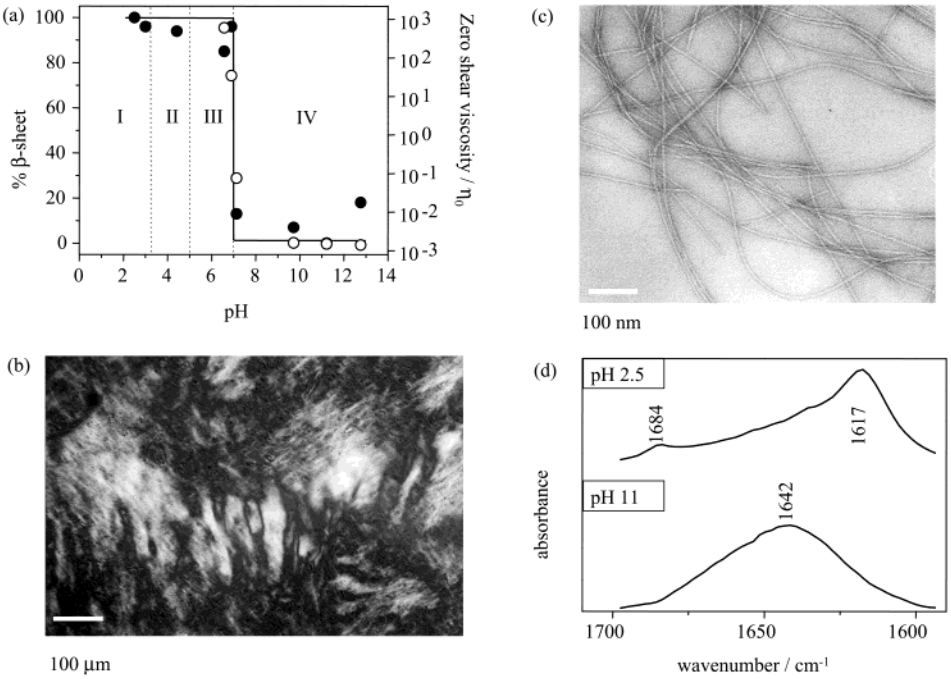

Figure 3. (a) Phase behavior of P_{11}-4 (c = 6.3 mM) as a function of pH (DCl/NaOD): I = nematic gel, II = flocculate, III = nematic fluid, IV = isotropic fluid. ○ = zero shear viscosity, and ● = % β-sheet determined using FTIR spectroscopy: the continuous line denotes the proportion of peptide in fibrils. The broken vertical lines separating regions I, II, and III denote approximate boundaries between different macroscopic fibrillar states, while that separating regions III and IV denotes a first-order nematic-to-isotropic transition. (b) Polarizing optical micrograph of a P_{11}-4 gel in water (c = 6.3 mM, pH = 3) showing a typical thick threadlike viscoelastic nematic texture (path length = 0.2 mm). (c) Transmission electron micrograph of a P_{11}-4 gel in water (c = 6.3 mM, pH = 3) showing semirigid fibrils and fibers. Micrographs were obtained after dilution to 20 μM and negative staining with uranyl acetate. (d) FTIR spectrum of amide I′ (mainly C═O stretching absorption) bands showing β-sheet conformation of P_{11}-4 nematic gel (c = 6.3 mM) in DCl at pH 2.5 (upper trace) and random coil state of P_{11}-4 isotropic fluid (c = 6.3 mM) in NaOD at pH 11 (lower trace).

centered at 1617 cm^{-1} and a weak band at 1684 cm^{-1}, a signature of the antiparallel β-sheet structure of fibrils.[15,16] This contrasts with the broad amide I′ absorption band centered at 1642 cm^{-1} observed for a solution at pH 11 (Figure 3d (lower trace)), a signature of the "unstructured" peptide which we have identified with the monomeric state (see Experimental Section). The nematic-to-isotropic fluid transition, as depicted in Figure 3a, occurs within the pH range 6.8−7.2. We note here that the transition occurs approximately three pH units higher than the pK (4.1) of free glutamic acid.

Further insight into the nature of the nematic-to-isotropic fluid transition can be obtained from rheological measurements (Figure 4). For samples in region IV (Figure 3a), the viscosity is comparable to that of pure water (10^{-3} Pa·s) and is independent of shear stress, characteristic of Newtonian fluids. This behavior is consistent with the FTIR results which have shown that peptide is entirely in its monomeric state in this pH range. For the sample at pH 6.6 in the fluid nematic state (region III), the viscosity exhibits a sigmoidal decrease with increasing shear stress, characteristic of a shear thinning viscoelastic fluid.[17,18] The samples in the biphasic region at pH 6.9 and 7.13 are seen to exhibit behavior intermediate to the nematic and isotropic fluid states. This is interpreted to arise from dispersions of droplets of isotropic fluid in a continuous nematic medium

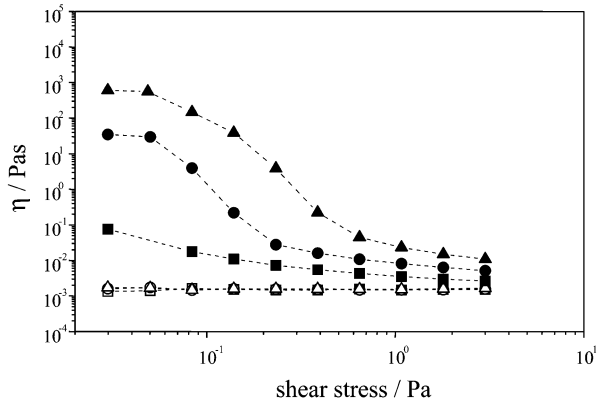

Figure 4. Shear viscosity η as a function of shear stress for 6.3 mM solutions of P_{11}-4 in the isotropic fluid state (pH 12.76, - -□- -; pH 11.22, - -○- -; and pH 9.72, - -△- -), nematic state (pH 6.6, - -▲- -), and biphasic region (pH 7.13, - -■- - and pH 6.9, - -●- -).

or, vice versa, in the biphasic interval. A sample in the nematic gel state at pH 2 (region I) was found to have a low finite yield stress (<0.025 Pa, the lowest accessible stress measurable with our instrument), making measurements of mechanical spectra impracticable. These gels are visually observed to be thixotropic with the gel recovering its self-supporting property approximately 20 min after being broken.

We find that we are able to "instantaneously" switch between nematic gel and isotropic fluid phases by addition of base or acid accordingly. Moreover, this process was found to be reversible. However, after typically four "pH jumps", we found that the concomitant increase in ionic strength led to flocculation of the gel which was then unresponsive to further additions of base.

(15) Krimm, S.; Bandekar, J. *Adv. Protein Chem.* **1986**, *38*, 181−364.
(16) Muga, A.; Mantsch, H. H.; Surewicz, W. K. *Biochemistry* **1991**, *30*, 2629−2635.
(17) (a) Evans, G. T. *J. Chem. Phys.* **1998**, *108*, 1570−1577. (b) Heyes, D. M.; Montrose, C. J.; Litovitz, T. A. *J. Chem. Soc., Faraday Trans. 2* **1983**, *79*, 611−635. (c) Muller, F. L.; Davidson, J. F. *Ind. Eng. Chem. Res.* **1994**, *33*, 2364−2367. (d) Heyes, D. M. *Mol. Phys.* **1986**, *57*, 1265−1282.
(18) Larson, R. G. *Structure & Rheology of Complex Fluids*; Oxford University Press: New York, 1999; Chapter 10, pp 461−463.

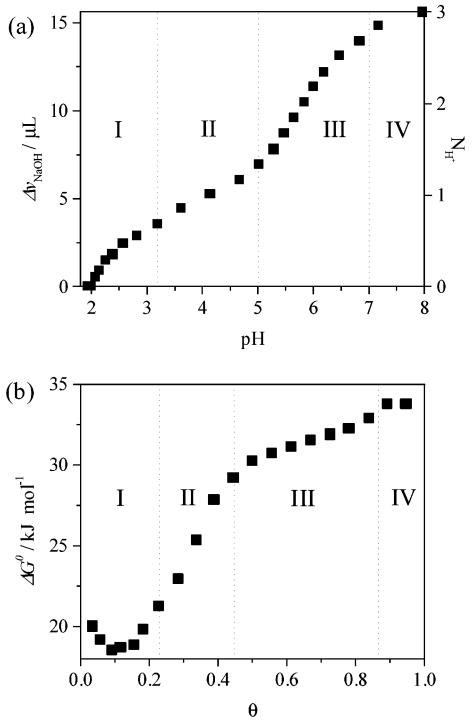

Figure 5. Titration curves of P_{11}-4: (a) The volume of 250 mM NaOH required to titrate glutamic acid side chains in 200 μL of 6.3 mM peptide solution as a function of pH. The corresponding number of dissociated protons N_{H^+} is given on the right-hand axis. I, II, III, and IV denote the regions corresponding, respectively, to nematic gel, flocculate, fluid nematic, and isotropic solution states. (b) The Gibbs free energy change $\triangle G°$ as a function of the degree of acid dissociation θ.

The existence of P_{11}-4 (6.3 mM) in four distinct states (I−IV in Figure 3a) between pH 2 and pH 13 leads one to surmise that these states are associated with distinctly different charged species of P_{11}-4 (Arg^+; Arg^+, Glu^-; Arg^+, $2Glu^-$; Arg^+, $3Glu^-$). This would require that all three Glu residues have distinct pK values. However, this is a gross oversimplification. This can be seen from results of the titration of a nematic gel of P_{11}-4 (pH 2) with 0.25 M NaOH solution (Figure 5a). The dissociation of protons is seen to occur over a wide band of pH values from 2 to 8, reminiscent of the titration behavior of proteins.

The behavior depicted in Figure 5a is characteristic of polyacids.[19] Proton dissociation from the glutamic acids embedded in fibrils is influenced by extensive electrostatic forces between γ-COO^- of Glu and the δ-guanidinium$^+$ groups of Arg in the tapelike substructure. Attractive forces essentially lower the acid pK to below that of the free peptide (ca. 4.1), while repulsive ones raise it to higher values.[20] The usual practice[20,21] is to define an apparent dissociation constant $pK = pH - \log_{10}(\theta/(1-\theta))$, where θ is the degree of dissociation, and to express the difference between pK and the value of the free monomeric peptide pK_0 by $\Delta pK = pK - pK_0$. Alternatively, we have chosen to use the relationship $pK = -\log_{10} K = \Delta G°/2.303RT$ to calculate the Gibbs free energy change $\Delta G°$ as a function of the degree of dissociation. The shape of the resulting titration curve in Figure 5b is qualitatively reminiscent of those

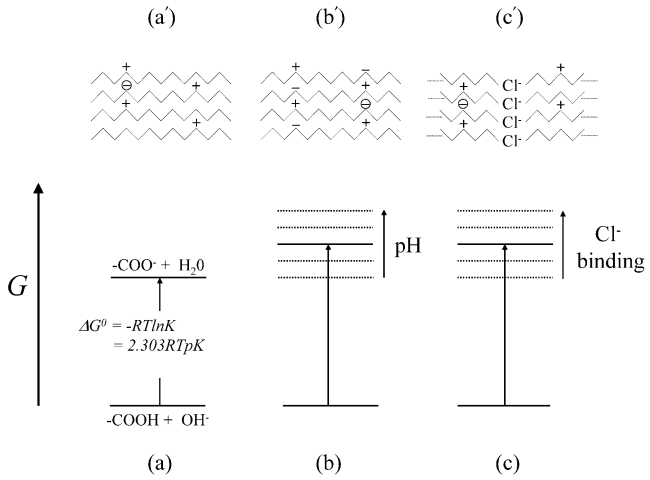

Figure 6. Schematic showing the free energy of deprotonation $\triangle G°$ of Glu in P_{11}-4: (a) deprotonation of the first glutamic acid at pH = 2.0, the resulting charge distribution [+ = Arg^+; − = Glu^-] along the peptide backbone is illustrated in part a′; (b) depiction of the effect of increasing electrostatic repulsion on $\triangle G°$ resulting from raising the pH value above 2.0 (region I); (c) depiction of the effect on $\triangle G°$ of Cl^- binding at the interface between the edges of neighboring fibrils at fiberlike junctions in nematic gel phases. In parts a′, b′, and c′, ⊖ denotes the glutamic acid deprotonation site associated with the transition depicted in parts a, b, and c, respectively.

observed experimentally for linear polyacids such as polyglutamic acid[19] and in corresponding Monte Carlo simulations.[21] Quantitative differences are to be expected to stem from the rigidity and complexity of the charge distribution within fibrils as compared to the linear, flexible polyacids. In particular, we note how below $\theta \approx 0.1$ the slope of the titration curve changes from positive to negative values. We might have expected $\Delta G°$ to have continued roughly linearly to $\theta = 0$, giving an intercept of 11.4 kJ mol^{-1}, the $\Delta G°$ for dissociation of glutamic acid in the +1 charged state of the peptide molecule (Figure 6a). The upward deviation of the titration curve at low θ (low pH values) is believed to be associated with the formation of fiberlike junctions and as such can throw light on the nature of gelation. Fiber formation is driven by the edge-on-edge attractive forces between tapes in adjacent fibrils across these junctions. These will undoubtedly involve hydrogen bonding between Gln in positions 1 and 2 and 10 and 11 and the acetyl and amide blocking groups as well as hydrophobic forces stemming from the acetyl CH_3 groups. The formation of these junctions at low pH may result from the attenuation of the electrostatic repulsive forces associated with the increase in ionic strength of the medium brought about by acidification with HCl. Concomitantly, the intercalation of Cl^- ions in the interface, that is, bridging Arg^+ in opposing tape-edge surfaces, may also result in significant contributions to the attractive forces. The binding of the Cl^- ions to proteins at pH ≤ 2 has been implicated in the refolding of proteins,[22] and there is also some evidence for Arg^+- - -Cl^-- - -Arg^+ salt bridges in proteins.[23] The increasing value of $\Delta G°$ as $\theta \rightarrow 0$ could be accounted for by electrostatic repulsive forces of the type Cl^-- - -COO^- (Figure 6c), consistent with the accumulation of Cl^- ions in the interface on addition of HCl.

In region III, repulsive electrostatic forces between COO^- acid groups in Glu^- would tend to destabilize fiberlike junctions.

(19) (a) Nagasawa, M.; Holtzer, A. *J. Am. Chem. Soc.* **1964**, *86*, 531−538. (b) Olander, D. S.; Holtzer, A. *J. Am. Chem. Soc.* **1968**, *90*, 4549.
(20) Edsall, J. T.; Gutfreund, H. *Biothermodynamics: The Study of Biochemical Processes at Equilibrium*; John Wiley and Sons Inc.: Chicester, U.K., 1983; Chapter 5, pp 157−209.
(21) Ullner, M.; Woodward, C. E. *Macromolecules* **2000**, *33*, 7144−7156.
(22) Fink, A. L.; Calciano, L. J.; Goto, Y.; Nishimura, M.; Swedberg, S. A. *Protein Sci.* **1993**, *2*, 1155−1160.

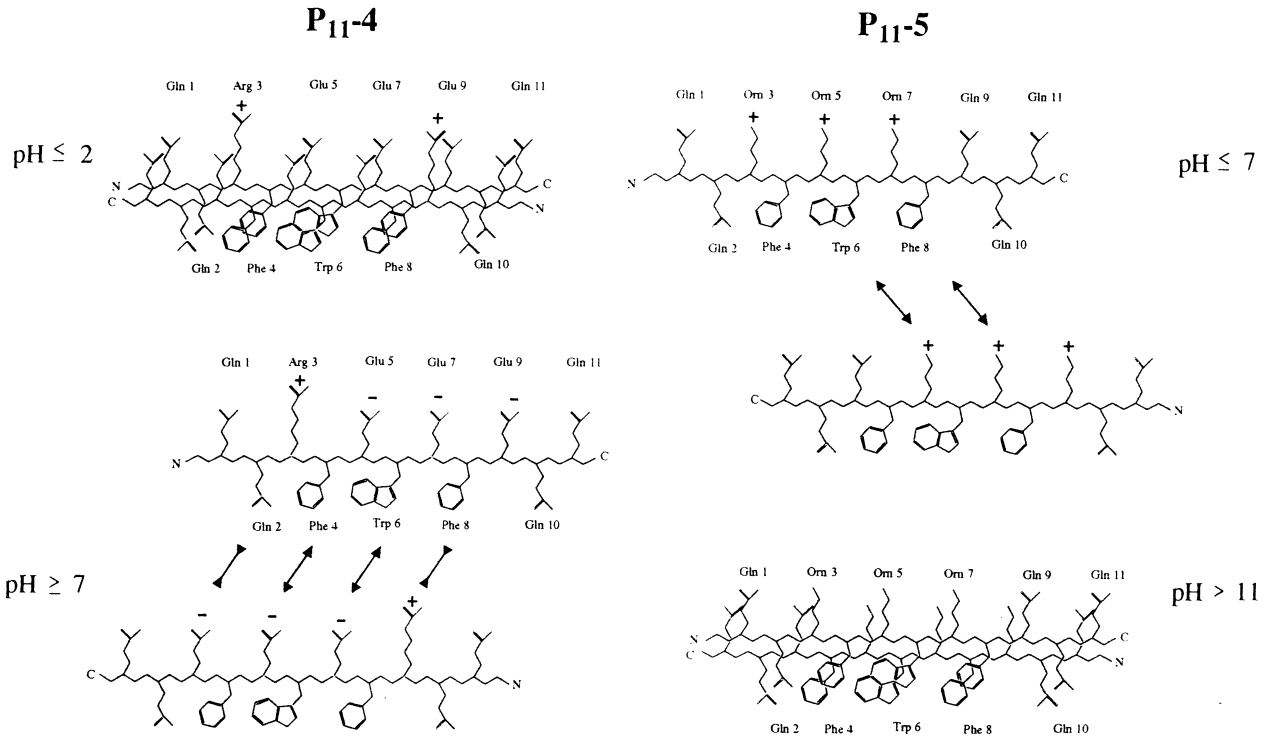

Figure 7. Ionization states of P_{11}-4 and P_{11}-5 at low and high pH values showing the side-by-side organization of peptides in tapelike substructures and in their dissociated monomeric states.

Support for this notion is seemingly obtained by the induction of a transition from a fluid nematic phase to a nematic gel in a sample $c = 6.3$ mM, pH = 6.0 by addition of NaCl to a concentration of 150 mM. This will screen the electrostatic repulsive forces between fibrils now with a net negative charge as well as increase the concentration of salt bridges of the kind Glu^-- - -Na^+- - -Glu^- [24] associated with possible intercalation of Na^+ in the interface. Further addition of NaCl induces flocculation of the gel.

We also note that gelation of low ionic strength samples in region III is induced at $c \geq 12.6$ mM. This is a direct consequence of raising the peptide concentration to values above the "critical fiber" concentration.

Switching between Nematic Gel at High pH and Isotropic Fluid State at Low pH. To demonstrate the universality of the pH triggering principle, a complementary peptide P_{11}-5 was designed to display the converse switching behavior to that of P_{11}-4, that is, to be in the monomeric state in acid solutions and in fibrillar aggregates in basic solutions (Figure 7). To achieve this, residues at positions 3, 5, and 7 in P_{11}-2 were changed to ornithine (Arg3 → Orn, Gln5 → Orn, Gln7 → Orn), and the glutamic acid at position 9 was changed to glutamine (Glu9 → Gln) (Table 1). Ideally, it would be appropriate to incorporate a residue that would be negatively charged at pH values greater than the apparent p*K* of Orn to prevent flocculation of fibrils at very high pH values. We have chosen not to do this here because the objective was solely to demonstrate the utility of pH switching to control the isotropic-to-nematic gel transition. However, it turns out that the reaction of CO_2 with the amino groups on deprotonated Orn at high pH values leads to formation of carbamate:[25]

$$RNH_3^+ \overset{-H^+}{\longleftrightarrow} RNH_2 \overset{+CO_2}{\longleftrightarrow} RNHCOOH \overset{-H^+}{\longleftrightarrow} RNHCOO^-$$

Repulsion from these negatively charged carbamate groups will be seen to provide stabilization of fibrillar dispersions.

Acidic solutions are Newtonian fluids of monomeric peptide, while above pH 7.8 fluid nematic phases occur at concentrations in excess of 0.9 mM and nematic gels, above 6.6 mM (comparable to the behavior of P_{11}-4). The pH dependence of a 13.1 mM solution is summarized in Figure 8a. The isotropic-to-nematic transition occurs within the pH interval 7.4−7.8, some 3 pH units below the pH observed for deprotonation of ornithine in peptide monomers.[26] A solution of pH = 7.6 displays nematic droplets with a radial director distribution (maltese cross when viewed between crossed polars), diameter ≈ 300 μm, dispersed in an isotropic fluid phase, indicative of the biphasic nature of the transition (Figure 8b). At pH ≤ 7.4, the peptide is in an unstructured state in solution (Figure 8d (lower trace)), while, at higher pH values, it is incorporated in semirigid fibrils (Figure 8c) in an antiparallel crossed β-configuration (Figure 8d (upper trace)). The maximum "diameter" of the fibrils is typically 8−12 nm, corresponding to 8−12 tapes.

(23) (a) Heinz, D. W.; Baase, W. A.; Dahlquist, F. W.; Matthews, B. W. *Nature* **1993**, *361*, 561−564. (b) Blaber, M.; Zhang, X. J.; Matthews, B. W. *Science* **1993**, *260*, 1637−1640. (c) Thoden, J. B.; Miran, S. G.; Phillips, J. C.; Howard, A. J.; Raushel, F. M.; Holden, H. M. *Biochemistry* **1998**, *37*, 8825−8831.

(24) (a) Fuentes-Prior, P.; Iwanaga, Y.; Huber, R.; Pagila, R.; Rumennik, G.; Seto, M.; Morser, J.; Light, D. R.; Bode, W. *Nature* **2000**, *404*, 518−525. (b) Larsen, T. M.; Benning, M. M.; Rayment, I.; Reed, G. H. *Biochemistry* **1998**, *37*, 6247−6255.

(25) (a) Schimming, V.; Hoelger, C.-G.; Buntkowsky, G.; Sack, I.; Fuhrhop, J.-H.; Rocchetti, S.; Limbach, H.-H. *J. Am. Chem. Soc.* **1999**, *121*, 4892−4893. (b) Edsall, J. T.; Wyman J. *Biophysical Chemistry, Volume 1*; Academic Press: New York, 1958; Chapter 10.

(26) Greenstein, J. P.; Winitz, M. *Chemistry of the Amino Acids*; John Wiley and Sons Inc.: New York, 1961; Chapter 4, p 486.

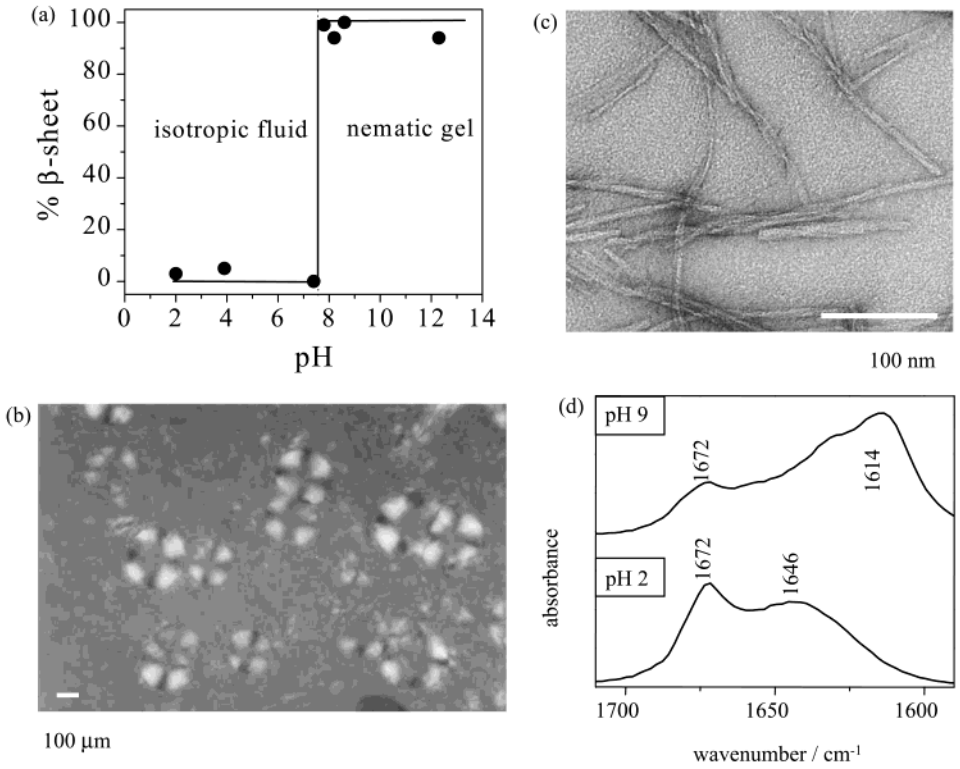

Figure 8. (a) Phase behavior of P_{11}-5 (c = 13.1 mM) as a function of pH (DCl/NaOD), showing the sharp transition from isotropic fluid to nematic gel states at pH 7.5. (b) Polarizing optical micrograph showing nematic droplets with a radial director distribution (maltese cross) dispersed in an isotropic fluid phase. (c) Transmission electron micrograph of a gel (pH 9, c = 13.1 mM) showing semirigid fibrils. (d) FTIR spectrum of amide I′ bands showing β-sheet conformation of P_{11}-5 in the nematic gel state (c = 13.1 mM, pH 9, NaOD), upper trace, and the random coil conformation in the isotropic fluid state (c = 13.1 mM, pH 2, DCl), lower trace.

The titration curve for P_{11}-5 (not reproduced here) is similar in shape to that for P_{11}-4, occurring over a wide band of pH values from 7.5 to 11. The onset of deprotonation occurs some 3 pH units below the pK (10.8) of free ornithine in solution. The decrease in apparent pK presumably arises from repulsive forces between Orn^+- - -Orn^+. The stability of the gel state across this entire pH interval is attributed to the stability of fiberlike junctions at these high peptide concentrations. Here, we expect a similar set of forces to prevail as in the case of P_{11}-4 except that anions X^- are now expected to be intercalated at the interface. We believe that the anion here is residual $CF_3CO_2^-$ from peptide synthesis and purification. The presence of $CF_3CO_2^-$ is indicated by an absorption band at 1672 cm^{-1} in the FTIR spectrum (Figure 8d). There is evidence for salt bridges of the kind Lys^+- - -X^-- - -Lys^+ in proteins.[27] The stability of the gel at the high pH limit is we believe a consequence of a net negative charge on the fibrils stemming from carbamate formation as indicated in the titration curve which reveals more than 3 equiv of titratable protons.

The pH dependence of the phase behavior of all the four peptides studied here are compared in Figure 9.

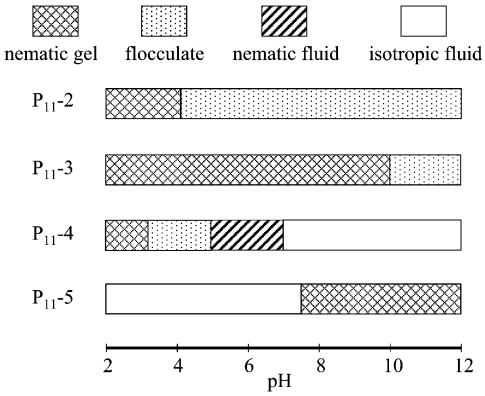

Figure 9. Summary of phase behavior of 11 amino acid peptides in aqueous solution as a function of pH. For P_{11}-2, P_{11}-3, and P_{11}-4, c = 6.3 mM, and for P_{11}-5, c = 13.1 mM.

Discussion

Structure of the Nematic Gel State. Our model for hierarchical peptide β-sheet self-assembly[4] predicts that fibrils will become entwined to form fibers above a critical peptide concentration c^*_{fiber} with the concentration of peptide in fibrils remaining invariant above this concentration. In the case of P_{11}-2, electron micrographs[1] suggest that fiber formation is quite random leading to the hypothesis that the fiberlike entanglements constitute the junctions in gel networks (Figure 10). While there is no evidence for distinct fibers, more the participation of fibrils in fiberlike entanglements, it could well be that the prevailing structure is metastable. These fiberlike junctions are easily broken by shear and can re-establish over time accounting for the low yield stress and thixotropic nature of the gels. The new observations reported here suggest that junction formation is promoted by (i) increasing peptide concentration and (ii) increasing ionic strength of the solution. The latter screens the electrostatic repulsion between fibrils allowing the edge-on-edge attraction between tapes in adjacent fibrils to dominate. These attractive forces involve hydrogen bonding and hydrophobic

(27) (a) Xie, P.; Parsons, S. H.; Speckhard, D. C.; Bosron, W. F.; Hurley, T. D. *J. Biol. Chem.* **1997**, *272*, 18558−18563.

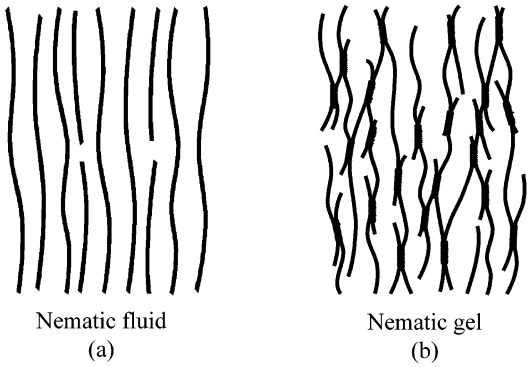

Figure 10. Schematic showing global arrangement of fibrils in nematic fluids (a) and the fiberlike junctions in nematic gel states (b).

forces and, quite likely, electrostatic forces arising from intercalation of counterions in the interface between adjacent tape edges. For example, for P_{11}-4 in region I, we believe Cl^- anions form salt bridges between the Arg^+ of which there is one per peptide molecule (Figure 8). In region III, there is a net negative charge per peptide of between 0.5 and 2.0 units and a cation is now required. The only contender is Na^+. However, the activity of Na^+ in the solutions studied is such that c^*_{fiber} is not attained. Adding NaCl to the solution of P_{11}-4 at $c = 6.3$ mM, we observe gelation sets in when a concentration of NaCl of 150 mM was reached. However, both the Na^+ concentration and ionic strength are increasing, and it is not practicable to distinguish between the two effects. In the case of P_{11}-5, for $c = 13.1$ mM, nematic gels are obtained throughout the pH range 7.8−13. In this case, an anion, $CF_3CO_2^-$, is likely to be involved in salt bridge formation between Orn^+ bridging the edges of tapes in adjacent fibrils.

Nature of the Nematic-to-Isotropic Phase Transition. The isotropic-to-nematic transition previously observed[4] with increasing concentration of P_{11}-2 in acid solution (pH 2) was shown to be consistent with a model of semirigid (rodlike) fibrils with hard-core excluded volume interactions and with the isotropic-to-nematic transition occurring at a volume fraction concentration $\phi_{IN} \approx 5.5D/P_{fibril}$, where D is the effective diameter of the fibril and P_{fibril}, its persistence length. The isotropic-to-nematic transition observed here on lowering the pH of a 6.3 mM solution of P_{11}-4 is, however, distinctly different in its nature. IR experiments have established that in the isotropic fluid state the peptide is present as the monomeric species, while in the nematic state it is present in elongated fibrils. That is, here the isotropic-to-nematic transition is governed by the reversible association of monomeric peptide molecules into fibrils. This is a simple two-state transition. The width of the nematic/isotropic coexistence region is determined by the pH interval of this transition. Here, it is quite narrow, occurring between pH 6.8 and 7.2, as implied by the rheology measurements (Figure 4). Optical microscopy (Figure 9b) reveals a similar isotropic-to-nematic coexistence interval for P_{11}-5. Single domain proteins undergo highly cooperative reversible unfolding transitions over comparable pH intervals.[28] The highly cooperative dissociation of fibrils as observed here stems from the regular crystal-like structure of the fibrils: they are comprised of stacks of twisted tapes. Within each tape, the peptide molecules are arranged linearly and the peptide−peptide interaction free energy ϵ_{tape} contains contributions stemming from long-range electrostatic forces between charged side chain groups. The deprotonation at a single Glu will therefore trigger long-range perturbations of ϵ_{tape}. This also explains the cooperativity of the transition and also its extreme sensitivity to additions of very small aliquots of base/acid.

The reduction in the value of ϵ_{tape} brought about by increasing the electrostatic repulsive force between neighboring peptides by raising pH would be expected to be reversible on addition of salt. Indeed, we find that addition of NaCl to a 6.3 mM solution of P_{11}-4 at pH 8.0 induces a fluid-to-nematic transition at a salt concentration of 150 mM. Thus, salt can be used in a complementary manner to pH to effect changes in the value of ϵ_{tape} and to switch between different macroscopic states. In effect, the pH at which fibrils dissociate into monomeric peptides will be raised by increasing the ionic strength of the solution. In the case of P_{11}-4, the upper limit to this behavior would be at pH 8 corresponding to dissociation of all glutamic acid protons (Figure 5a). Adding an additional Glu residue would extend this upper limit.

We note here that the need for the order of one unit of net positive or negative charge per peptide molecule to prevent flocculation of dispersions of fibrils is indicative of the stabilization through electrical double layer forces. This will require the presence of a diffuse layer of counterions surrounding each fibril. In which case, it raises the fascinating issue as to the location within the fibrils of any adsorbed counterions.

Kinetics of the Switching Process. One of the surprising observations in the work presented here is the speed (seconds) of switching between the isotropic fluid and nematic state and its reversibility, albeit after switching three to four times between low and high pH states the build-up in ionic strength resulting from the added acid and base led to screening of the electrostatic repulsion between fibrils and their eventual flocculation. This is in marked contrast to the normal route to fibrils starting from the dissolution of monomeric lyophilized peptide at pH 2 which is a much slower process, typically taking days or weeks to complete. We believe this is a consequence of the different kinetic pathways involved. In a separate study[4] of the self-assembly of P_{11}-2 at pH 2, it has been found that (with increasing peptide concentration) the sequence of self-assembling structures is random coil → short tapes → ribbons → fibrils → fibers (Figure 1). The transition from one structure to the next higher order structure occurs at a set of well-defined critical concentrations, above which the size and concentration of the lower order structures are fixed. The actual transition rates between different aggregate structures are extremely slow. This stems from the strength and multiplicity of the peptide−peptide interactions involved. The high tape scission energy $\epsilon_{tape} \approx 24.5k_BT$ of P_{11}-2 ensures that peptide dissociation from free ends of tapes, ribbons, or fibrils is a rare event: the effective dissociation rate $\tau_0^{-1} \exp(-\epsilon_{tape}) \approx 10^{10}\tau_0^{-1}$ corresponds to a dissociation time τ of the order of one second for $\tau_0 \approx 100$ ps (τ_0 is a typical diffusion time of a peptide "rod" over a distance of 0.1 nm). The energy required to break a ribbon, $\epsilon_{sc,ribbon} = 2\epsilon_{tape} \approx 50k_BT$, gives rise to a scission (breaking) time of a ribbon of $\tau_0 \exp(2\epsilon_{tape}) \approx 10^4$ years. The scission energy for a P_{11}-2 fibril comprised of four ribbons (eight single tapes) is $\epsilon_{sc,fibril} = 8\epsilon_{tape} \approx 200k_BT$, comparable to covalent bond energies. The conversion of

(28) Creighton, T. E. *Proteins − Structures and Molecular Properties*, 2nd ed.; W. H. Freeman and Company: New York, 1993; Chapter 7, pp 287−291.

ribbons to fibrils requires ribbons to wind around each other, which is likely to be highly hindered in a dense system of entangled ribbons. More likely, they dissociate into smaller fragments followed by reassembly; this process will be slow due to the high $\epsilon_{sc,ribbon}$. Thus, the gradual dissolution of lyophilized solid will result in a gradual increase in the peptide concentration in solution which will inevitably lead to the nucleation of tapes or ribbons. Their subsequent conversion to fibrils is expected to be an exceedingly slow process. In contrast, in the case of P_{11}-4, switching from pH > 7.0 to pH < 3.2 changes the net charge from −2 to +1 per peptide (Figure 8a) which increases ϵ_{tape} and consequently shifts the critical fibril concentration to a value below the actual peptide concentration with the result that the monomeric peptide undergoes rapid, direct, cooperative self-assembly into fibrils (see scheme in Figure 1). We also found, for P_{11}-2 at pH 2, that the slow tape-to-ribbon path can be circumvented by seeding the monomeric solution with preformed fibrils, thus reproducing the behavior reported for many amyloid forming peptides.[30] The speed of the reverse process, that is, dissociation of fibrils into monomers (when, in the case of P_{11}-4, the pH is switched to values in excess of 7.2), is governed simply by the effective "melting" of typically 8.0 nm wide fibrils. A detailed mechanistic study of the kinetic pathways governing the self-assembly process in these model peptide systems will be instructive and help to establish a fundamental understanding of the mechanism of the pH switching process.

Conclusions

The principles of β-sheet tapelike self-assembly established herein and by our previous studies[2−4] are beginning to lay the foundations for the production of a new class of soft−solidlike nanostructured materials. Precise control of the nanostructures provides control of the mesostructure and, in turn, the macroscopic properties of these materials. Their eventual deployment will, by necessity, rest on the development of low cost routes for the production of peptides from transgenic animals and plants.[31] Their novelty stems from the involvement of self-assembly and the opportunity to control this process by external triggers. Here, we have demonstrated the use of pH switching for this purpose, but other chemical, electrical, and optical triggers can be envisaged. Biocompatibility and biodegradability are also attractive properties for prospective biomedical applications. For example, nematic gels could find use as bioscaffolds to control the shape and alignment of cells in tissue engineering. Nematic states could also be used as matrixes for separation of chiral molecules as well as to orient biomolecules for spectroscopic (NMR) studies. Of practical importance, pH switching provides a way for the direct and controlled production of nematic fluid phases or gels from monomeric peptide, avoiding any intermediate structural traps. It also provides a means for encapsulation and controlled release of large biomolecules or cells from gels. Artificial proteins having a leucine zipper element which can form coiled-coil aggregates in response to changes in pH have also been proposed for the reversible control of hydrogels.[32] The use of small peptides for this purpose has the advantages of ease of synthesis and speed of switching, as demonstrated here and in related studies of 12 amino acid peptides.[32] Notwithstanding any potential applications of these materials, these studies of β-sheet tapelike self-assembly are exposing principles that will govern the assembly not only of small peptides but also of larger protein aggregates.

Experimental Section

Synthesis and Purification of Peptides. Peptides were synthesized using standard solid-phase 9-fluorenylmethoxycarbonyl (Fmoc) chemistry. The peptides were assembled on NovaSyn TGR/PEG-PS (poly(ethylene glycol)−polystyrene) resin, incorporating a linker to generate the C-terminal amide upon cleavage of the peptide from the resin. Fmoc-amino acids were C-terminally activated using [2-(1*H*-benzotriazol-1-yl)-1,1,3,3-tetramethyluronium hexafluorophosphate] (Hbtu) with diisopropylethylamine (DIPEA). The resin-bound peptide was N-terminally acetylated by reaction with 0.3 M acetic anhydride−0.03 M pyridine in dimethylformamide (DMF) (10 min at room temperature). Cleavage of the peptide from the resin and deprotection of amino acid side chains were achieved by incubation for 3 h in trifluoroacetic acid (TFA) containing 1% (w/v) phenol, 2% (v/v) water, 4% (v/v) ethane-1,2-dithiol, and 2% (v/v) anisole. The peptide was precipitated with diethyl ether, centrifuged, and washed a further 4 times with diethyl ether. The diethyl ether was evaporated, and the peptide dissolved in water for purification. P_{11}-2, P_{11}-3, and P_{11}-5 were purified by reversed-phase HPLC using a 20%−40% water−acetonitrile gradient in the presence of 0.1% TFA which gave baseline resolution of peptide fractions. MALDI-TOF mass spectrometry showed single peaks (>95% purity) at the expected molecular weights (P_{11}-2, *m*/*z* 1594; P_{11}-3, *m*/*z* 1593; P_{11}-5, *m*/*z* 1523). P_{11}-4 was purified by reversed-phase HPLC using 0.1% ammonia in water as buffer A and 10% buffer A in acetonitrile as buffer B. MALDI-TOF mass spectrometry showed a single peak (>95% purity) at the expected molecular weight *m*/*z* 1596.

Sample Preparation. Samples were prepared by dissolving a known mass of lyophilized peptide in the appropriate volume of D_2O, at concentrations in excess of the nominal critical fiber concentration. The pH (uncorrected meter readings were recorded) of the solutions was controlled by addition of appropriate amounts of either hydrochloric acid solution (DCl) or sodium hydroxide solution (NaOD). Typically, the pH of solutions studied were between 2 and 13. This precluded the use of standard buffer solutions. Samples were mixed for 15 s, sonicated for 15 min, and left to equilibrate at room temperature for 2 days.

FTIR Spectroscopy. Spectra were recorded on a Perkin−Elmer 1760X FTIR spectrometer. Samples were placed between CaF_2 crystals separated by a 50 μm Teflon spacer. Spectra were averages of four scans, recorded with a resolution of 4 cm^{-1} at room temperature, and have had the blank solvent spectrum subtracted. The proportion of peptide in β-sheet aggregates was calculated by deconvolution of the experimental spectra and associated with independent time-resolved fluorescence anisotropy (TRFA) measurements (unpublished work, in collaboration with Dr. M. Martin-Fernandez, Daresbury lab). TRFA data has shown that nematic gels of P_{11}-4 at pH 2 contain predominantly β-sheet polymers with as little as 2% monomeric peptide and that isotropic fluids at pH 9 contain purely monomeric peptide. Spectra obtained from nematic gels are therefore taken to be characteristic of all peptides in a β-sheet conformation, while spectra from isotropic fluids are taken to be characteristic of peptides in a monomeric random coil state, and then all spectra are normalized.

Rheology. Viscometry measurements were performed using a Bohlin CVO constant stress rheometer in the constant stress mode. A Mooney Ewart geometry was employed where the bob length and radius were 12.9 and 12.5 mm, respectively, the cone angle was 1.8°, and the cup

(29) (a) Come, J. H.; Fraser, P. E.; Lansbury, P. T., Jr. *Proc. Natl. Acad. Sci. U.S.A.* **1997**, *90*, 5959−5963. (b) Harper, J. D.; Lansbury, P. T., Jr. *Annu. Rev. Biochem.* **1997**, *66*, 385−407.
(30) Artsaenko, O.; Kettig, B.; Fiedler, K.; Conrad, K.; During, K. *Mol. Breed.* **1997**, *4*, 313−319.
(31) Petka, W. A.; Harden, J. L.; McGrath, K. P.; Wirtz, D.; Tirrell, D. A. *Science* **1998**, *281*, 389−392.
(32) Caplan, M. R.; Moore, P. N.; Zhang, S.; Kamm, R. D.; Lauffenburger, D. A. *Biomacromolecules* **2000**, *1*, 627−631.

radius was 12.95 mm. Approximately 700 μL of sample was loaded into the cup using a syringe, after which the bob was lowered to a predetermined level and any excess sample removed. To prevent solvent evaporation, 1cS silicone fluid (Dow Corning) was floated over the exposed surface area of the sample. The silicone fluid and sample were immiscible, and there was no effect on the sample chemistry; control tests showed the silicone fluid did not affect the sample rheology. Viscometry measurements were taken over a range from 0.03 to 3 Pa, with 5 points per decade and a measurement time of 60 s per point. The sample temperature was kept at a constant 20 $\pm$ 0.1 °C using a circulating water bath surrounding the cup. The sample was allowed to equilibrate for a minimum of 20 min prior to any testing and between test runs.

Transmission Electron Microscopy (TEM). Samples were examined using a Phillips CM10 TEM at 100 kV accelerating voltage. Gels were diluted to a peptide concentration of 20 μM immediately before application to a glow-discharged, carbon-coated, 400 hexagonal mesh copper grid. The grid was deposited on top of the 20 μL sample droplet for 1 min, excess sample drained, and then the grid was introduced to a droplet of uranyl acetate solution (4% w/v in water) for 20s.

Optical Microscopy. Optical micrographs were recorded using an Olympus BH-2 microscope. Samples were contained in optical capillaries with a path length of 0.2 mm and viewed through cross-polarizing filters. The microscope was calibrated using a graticule.

pH Titrations. P_{11}-4 was dissolved in 10 mM HCl at a peptide concentration of 6.3 mM and adjusted to pH 2 using concentrated HCl solution. The nematic gel formed was titrated with 1 μL additions of 250 mM NaOH, stirred for 30 s, and left for 1 min after which the constant pH meter reading was recorded. The results of titrations are presented as the difference (Δv_{NaOH}) between titrations in the presence and absence of peptide in solution. P_{11}-4 has 3 titratable side chains in the pH range 2−12; the end-point of the titration was therefore indicated when 3 molar equiv of NaOH had been added. pH was measured to $\pm$0.01 pH units using a Whatman Precision Instruments CD72O pH meter.

Acknowledgment. We thank the UK Engineering and Physical Sciences Research Council, the Wellcome Trust and Schlumberger Cambridge Research for financial support, and the Royal Society for the award of a University Research Fellowship to A.A. S.E.R. is a BBSRC professorial fellow.

JA021047I